ARTICLE

Supporting Information

Multi-dimensional Dynamic Fluorescence Readout from Laser Engineered In_2O_3 Nanowire Micropattern

Eng Tuan Poh,[ab] Yung Zhen Tan,[c] Justin Boon Shuan Neo,[c] Chee How Ong,[c] Azianty Saroni,[d] Zheng Zhang,[e] Jianhui Li,[b] Boon Tong Goh,*[d] Chorng Haur Sow*[b]

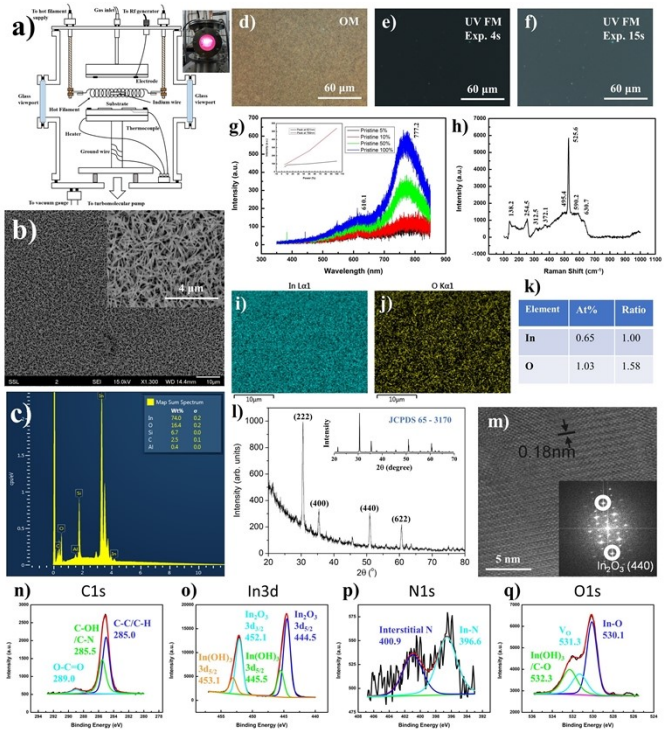

Figure S1. Production and basic characterization of pristine In_2O_3 nanowires. a) Schematic layout of RF plasma – assisted evaporation chamber utilized for In_2O_3 nanowire production. Inset: Photograph image of instrument during the plasma – assisted evaporation process. b) Uniform nanowire distribution under SEM imaging. Inset: Higher magnification image demonstrating single wire uniformity and dimensions. c) Corresponding EDX analysis output for dedicated SEM area in b). d) OM bright field image of nanowire distribution, along with corresponding FM images (under UV light excitation) with e) 4s, f) 15s exposure time. g) Laser power variable PL spectrum profiles of nanowire array under 325 nm excitation. Inset: Intensity to laser power (%) correlation for the respective peaks at 621.3 and 769.1 nm. h) Acquired Raman spectrum of the nanowire array under 532 nm excitation. i, j) Selected large area EDX mapping for the In_2O_3 nanowire sample of elemental signals i) In Lα and j) O Kα lines, providing a corresponding k) compositional ratio close to In_2O_3 formulae ratio. l) XRD profile and m) HRTEM imaging of In_2O_3 nanowires. Inset: Complementary SAED crystallograph. n-q) XPS spectra for the respective elements n) C1s o) In3d p) N1s q) O1s.

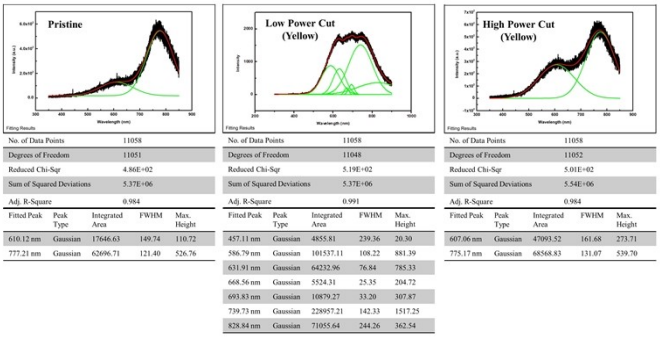

Figure S2. Fitting parameters for PL peak deconvolution under variable laser intensity modification. PL spectrum and fitting statistics for pristine sample (left), sample region of yellow fluorescence induced by low intensity (low lens NA) laser modification (middle), and sample region of reduced emission from higher intensity (high lens NA) laser modification (right).

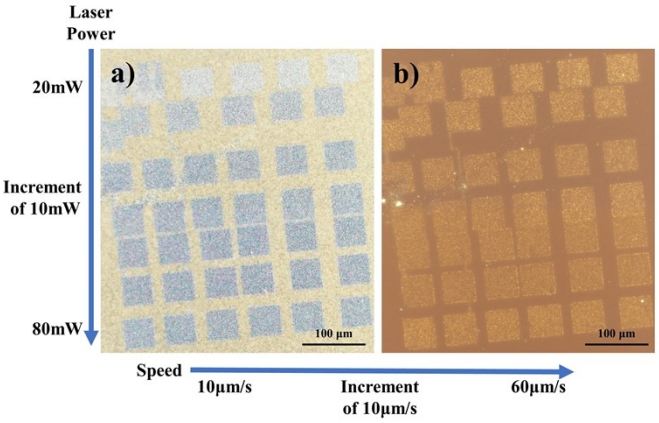

Figure S3. Parameter variation of laser modification under low laser intensity. a) OM bright field display of low intensity (low lens NA) laser raster array under influence of laser power and laser speed permutations. b) Corresponding FM overview of laser raster array in a). For both images: vertical top down – laser power variation in increments of 10 mW, from 20 mW to 80 mW; horizontal left right – variations in laser raster speed in increment of 10 µm/s, from 10 µm/s to 60 µm/s.

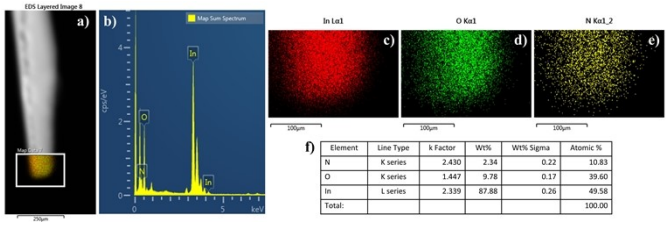

Figure S4. TEM EDX elemental analysis of nanowire tip composition. a) TEM image of selected nanowire, with EDX analysis region demarcated under white boxed region. b-e) Corresponding elemental analysis spectrum and various elemental maps for the respective c) In Lα, d) O Kα and e) N Kα line signals. f) Overall composition ration from the region elemental analysis.

Through the acquired atomic % of the various elements, we can determine the excess In present based upon the assumption that the N and O content exists only in the respective InN and In_2O_3 forms.

InN: 10.83% N → 10.83% In required

In_2O_3: 39.60% O → 26.40% In required

Total In content – In content in InN and In_2O_3 = 49.58% – (10.83% + 26.40%)

= 12.35% excessive In content

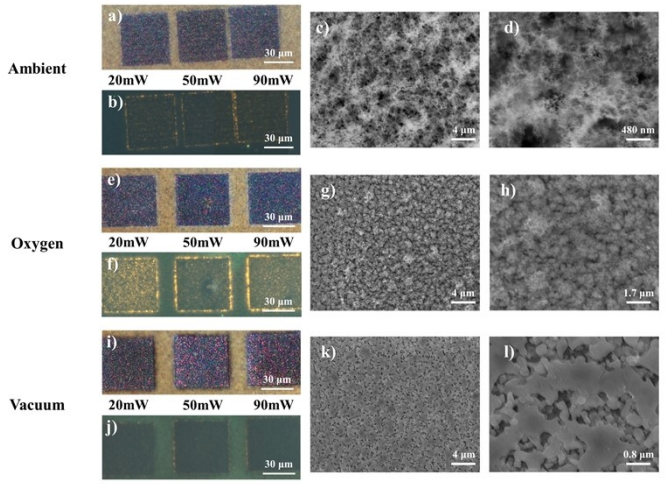

Figure S5. Nano-morphological features from high intensity (high lens NA) laser modification of samples under controlled environments. a) OM of nanowire domains, with its corresponding b) FM images under ambient condition laser irradiation. c) SEM and d) higher magnification SEM images of laser modified regions, highlighting the nanofibrous networks. e) OM of nanowire domains, with its corresponding f) FM images laser engineering under high oxygen content. g) SEM and h) higher magnification SEM images of laser modified regions, highlighting the fibrous cluster morphologies. i) OM of nanowire domains, with its corresponding j) FM images after laser alterations under vacuum conditions. g) SEM and h) higher magnification SEM images of laser modified regions, highlighting the melted particle morphology.

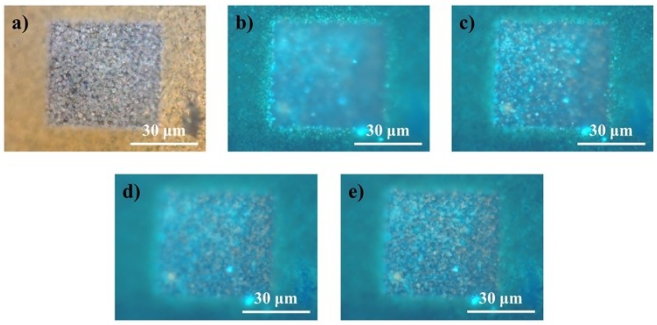

Figure S6. Sample fluorescence distribution with fluorescence microscope z-axial variation. a) OM bright field display of sample under low intensity (low lens NA) laser modification. b) Corresponding FM overview of laser modified region at highest z-focus. Surrounding unmodified nanowire domains in clear focus. c-e) Subsequent z-focus downward adjustment for sample fluorescence distribution profile: c) top layer focus of blue wire edges d, e) low height layer focus of underlying yellow fluorescence regions.

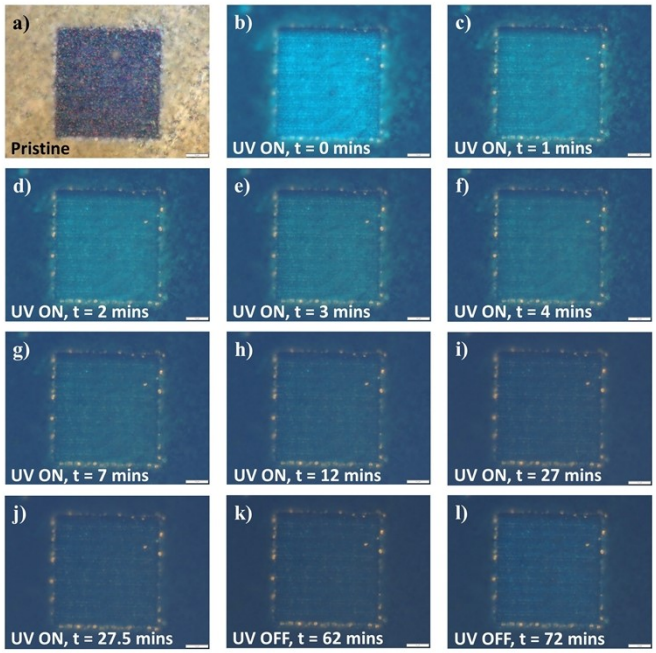

Figure S7. Sample fluorescence evolution under time-varied UV exposure ON-OFF. a) OM layout of high intensity (high lens NA) sample laser modified region after prolonged ambient exposure. b-j) Corresponding time points across UV exposure duration and influence on sample fluorescence – b) t = 0 min c) t = 1 mins d) t = 2 mins e) t = 3 mins f) t = 4 mins g) t = 7 mins h) t = 12 mins i) t = 27 mins j) t = 27.5 mins, demonstrating decreasing blue component with increased exposure time. k, l) Corresponding time points after cut-off of UV exposure and effect on sample fluorescence – k) t = 62 mins l) t = 72 mins, demonstrating the recovery of the blue fluorescence component.

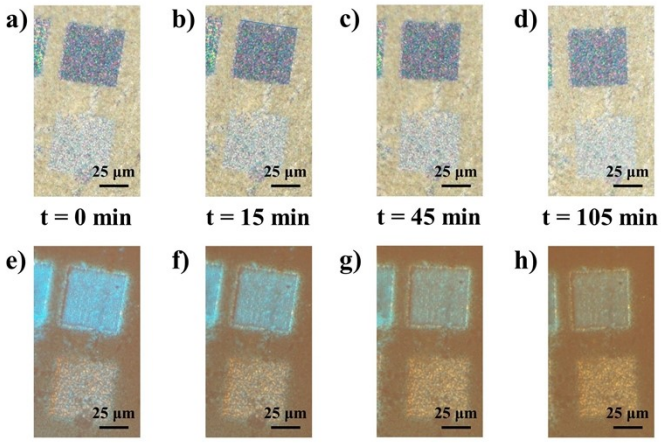

Figure S8. Sample fluorescence evolution under thermal annealing conditions. a-d) OM bright field layouts comprising sample squares modified from high intensity (top, high lens NA) and low intensity (bottom, low lens NA) laser exposure, across different time points of ambient thermal annealing (90°C) – a) t = 0 mins b) t = 15 mins c) t = 45 mins d) t = 105 mins. e-h) Corresponding FM layout for the same set of samples at different time points of ambient thermal annealing process - e) t = 0 mins f) t = 15 mins g) t = 45 mins h) t = 105 mins. Trend show the decline in blue contributions for all samples with increasing annealing time.

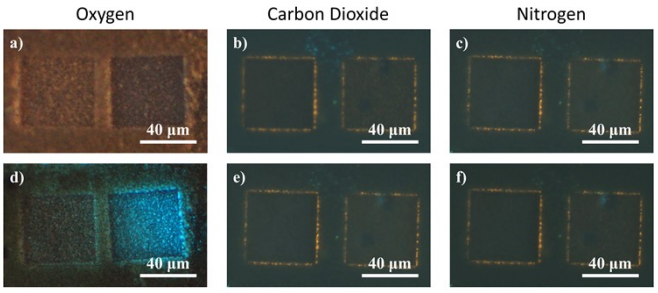

Figure S9. Environmental exposure parameters – gaseous source exposure reference controls. a-c) FM images of fresh laser altered samples (t = 0 hr) before emplacement within the respective gas chamber environments a) oxygen b) carbon dioxide c) nitrogen. d-f) Corresponding FM images of fluorescence square domains after extended exposure (t = 12 hr) amidst respective d) oxygen e) carbon dioxide f) nitrogen environments.

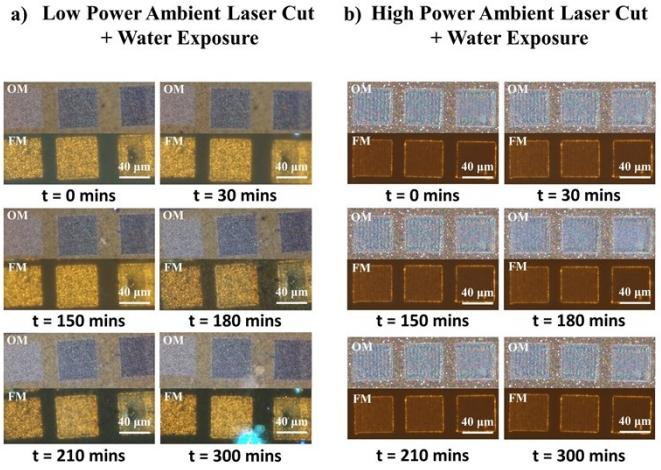

Figure S10. Environmental exposure parameters – water exposure reference controls. a) OM and FM images of ambient low intensity (low lens NA) laser modified sample progressively monitored over a range of prolonged water vapor exposure (t = 0 min, 30 mins, 150 mins, 180 mins, 210 mins, 300 mins). b) OM and FM images of ambient high intensity (high lens NA) laser modified sample progressively monitored over a range of prolonged water vapor exposure (t = 0 min, 30 mins, 150 mins, 180 mins, 210 mins, 300 mins).

Table S1. Summary of past literature works pertaining to In_2O_3 nanostructures and related PL emissions.

No.	Nanostructure (In_2O_3)	λ_{ex} (nm)	λ_{em} (nm)	Emission Mechanism / Species	Ref.
1	Cubic phase thin film	364	Orange, Broad, 400-800	Oxygen deficiencies	52
2	Nanowire array (AAO)	250	Blue, Broad, 300-600	V_O^+	53
3	Nanowire array (AAO)	274, 305	Blue, Sharp, 385-410	$V_O^+ (e^-) + h^+ \rightarrow h\nu$	54
4	Nanowires	382	Broad, 425-455	V_O^+	55
5	Nanowires	260 325	Blue, Broad, 300-600 Blue Broad, 390-480	$(V_{In} - V_O)^o + V_O^o \rightarrow$ $(V_{In} - V_O)' + V_O^+ + h\nu$	56, 57
6	Nanowires	254	Blue, Broad, 350-650	$V_O^+ (e^-) + h^+ \rightarrow h\nu$	58
7	Nanowires	330	Blue, 426, shoulder 406, 450	$V_O^+ (e^-) + h^+ \rightarrow h\nu$	59
8	Nanowires	325	Orange, Broad, 450-800	Orange: V_O Others (UV, blue, green, NIR): nanostructure, impurity, confinement	60
9	Ultrathin Nanowires	325	Green, Broad, 440-620	Deep donor V_O, Excitons, defect bound excitons and donor acceptor pairs	61
10	Nanowires on thin film	266, 375	Orange, Broad, 496-827 Blue, Sharp, 365-400	Blue: Exciton, defect bound excitons and donor acceptor pairs Orange: $V_O^+ (e^-) + V_{In}''/(V_O\text{-}V_{In})' (h^+) \rightarrow h\nu$	62
11	Nanowires, Nanobelts	325	Orange, Broad, 450-900	$V_O^+ (e^-) + h^+ \rightarrow h\nu$ Deep V_O or surface In	63–66
12	Nanowhiskers	325	Blue, Broad, 350-620 Yellow, Sharp, 500-800	Blue: $V_O^o (e^-) + (V_{In} - V_O)^o$ Orange: $V_O^+ (e^-) + VB/V_O^{++} (h^+)$	34
13	Nanofibers, Hollow Nanotubes	250	Blue, Broad, 400-700	Deep donor V_O	67, 68
14	Nanotubes	325	Blue, Broad, 385; Green + Orange, Broad, 537, 630	Blue: Near band edge Green: V_O Orange: In_i	69
15	Nanocones	390	Orange, Broad, 450-750 NIR, 800-950	Broad: $V_O^+ (e^-) + V_O' (h^+) \rightarrow h\nu$ NIR not accounted for	70
16	In@In_2O_3 core shell nanowires	325	Red, Broad, 500-1000	Blue: Band edge emission; Yellow: In_{i_a}; Red: In_{i_c}; V_O^+ - In_i	71
17	Short nanorods	300	Blue, Broad, 380-550	Near band edge emission	72
18	Nanotowers	325	Yellow, Broad, 460-750	$V_O^+ (e^-) + VB/V_O^{++} (h^+)$	73
19	Nanocrystals	234	Blue, Sharp, 400-450; shoulder 350-400	Quantum confinement	74
20	Octahedrons	325	Yellow, Broad, 500-850	Variable defect species: V_O^+, In_i^{2+}, O_{In}, V_{In}, O_i, In_i^{3+}	75
21	In_2O_3 and H-In_2O_3 nanoclusters	280	Blue, Sharp, 320-500; Green, Broad, 500-650	Blue: $V_O^o (e^-) + VB (h^+)$ Green: $CB (e^-) + V_O^+ (h^+)$	76